HHS Public Access

Author manuscript

Ocul Surf. Author manuscript; available in PMC 2024 April 01.

Published in final edited form as:

Ocul Surf. 2023 April ; 28: 99–107. doi:10.1016/j.jtos.2023.02.006.

Novel Characterization of CXCR4 expressing cells in uninfected and herpes simplex virus-1 infected corneas

Pratima Krishna Suvas[1], **Mizumi Setia**[1], **Mashidur Rana**[1], **Anish Chakraborty**[1], **Susmit Suvas**[*,1]

[1]Department of Ophthalmology, Visual and Anatomical Sciences, Wayne State University School of Medicine, Detroit, MI

Abstract

Purpose: To characterize CXCR4-expressing cells in uninfected and herpes simplex virus-1 (HSV-1) infected corneas.

Methods: The corneas of C57BL/6J mice were infected with HSV-1 McKrae. The RT-qPCR assay detected CXCR4 and CXCL12 transcripts in uninfected and HSV-1-infected corneas. Immunofluorescence staining for CXCR4 and CXCL12 protein was performed in the frozen sections of herpes stromal keratitis (HSK) corneas. Flow cytometry assay characterized the CXCR4-expressing cells in uninfected and HSV-1-infected corneas.

Results: Flow cytometry data showed CXCR4 expressing cells in the separated epithelium and stroma of uninfected corneas. In the uninfected stroma, CD11b+F4/80+ macrophages are the predominant CXCR4-expressing cells. In contrast, most CXCR4 expressing cells in the uninfected epithelium were CD207 (langerin)+, CD11c+, and expressed MHC class II molecule, documenting the Langerhans cells (LCs) phenotype. After corneal HSV-1 infection, CXCR4 and CXCL12 mRNA levels increased significantly in HSK corneas than in uninfected corneas. Immunofluorescence staining showed CXCR4 and CXCL12 protein localization in the newly formed blood vessels in the HSK cornea. Furthermore, the infection resulted in LCs proliferation, causing an increase in their numbers in the epithelium at 4 days post-infection (p.i.). However, by 9-day p.i., the LCs numbers declined to the counts observed in naïve corneal epithelium. Our results also showed neutrophils and vascular endothelial cells as the prominent CXCR4-expressing cell types in the stroma of HSK corneas.

Conclusions: Together, our data demonstrate the expression of CXCR4 on resident antigen presenting cells in the uninfected cornea and on infiltrating neutrophils and newly formed blood vessels in the HSK cornea.

[*]Corresponding author Dr. Susmit Suvas, 7233 Scott Hall, Department of Ophthalmology, Visual and Anatomical Sciences and Department of Biochemistry, Microbiology and Immunology, Wayne State University School of Medicine, Detroit, MI, Phone: 313-577-9820, Fax: 313-577-3125, ssuvas@med.wayne.edu.

Keywords

Langerhans cell; cornea; chemokine receptor; herpes simplex virus

Introduction

The naïve cornea is an avascular tissue but is well-reported to harbor antigen-presenting cells (APCs) [1]. These APCs are stratified in the different layers of the naïve cornea. Among APCs, CD11c+ dendritic cells are reported in the basal layer of the corneal epithelium [2], whereas the CD45+CD11b+ resident macrophages are shown in the corneal stroma of uninfected mouse cornea [3]. Similar stratification of APCs is noted in the human corneas. CD207+ Langerhans cells (LCs), a subpopulation of dendritic cells, are shown in the basal layer of the corneal epithelium, and CD68+ macrophages are reported in the anterior stroma of normal donor human corneas [4]. Although the functional significance of corneal APCs is not entirely understood, they are shown to mobilize to the site of infection upon corneal herpes simplex virus-1 (HSV-1) infection [4]. The factors that regulate the homing of these APCs in naïve cornea and their migration upon corneal HSV-1 infection are not fully understood.

Chemokine receptors are G-protein coupled receptors interacting with structurally similar protein molecules named chemokines [5]. The interaction between chemokines and chemokine receptors activates intracellular signaling pathways that play an essential role in homing, migration, proliferation, and survival of chemokine receptor-expressing cells [6-8]. CXCR4 is widely expressed among chemokine receptors and regulates physiological and pathological conditions [9, 10]. CXCR4 protein is evolutionary conserved, and the human and mouse CXCR4 share 89% similarity [11, 12]. The canonical chemokine ligand of CXCR4 is CXCL12, also known as stromal cell-derived factor-1 alpha (SDF-1α) [13]. CXCR4-SDF-1α signaling is known to play an important role in the homing of immune cells into bone marrow [14, 15]. A recent study has shown CXCR4-mediated recruitment of CD11c+ conventional dendritic cells in suture-induced corneal inflammation [16]. Similarly, the CXCR4-SDF-1α axis is reported to regulate hem-and lymphangiogenesis in sutured corneas in mice [17]. Even though the role of CXCR4 signaling is shown in sterile corneal inflammation, little is known about the characterization of CXCR4-expressing cells in uninfected and HSV-1-infected corneas.

In the current study, we detected CXCR4-expressing cells in the separated epithelium and stroma from uninfected murine corneas by flow cytometry. In epithelium, most CXCR4-expressing cells bear the signature of LCs, whereas most stromal CXCR4+ cells exhibit macrophage phenotype. Corneal HSV-1 infection resulted in a transient increase in CXCR4-expressing LCs in the epithelium. In addition to resident APCs, CXCR4 expression was noticed on infiltrated neutrophils and newly formed blood vessels in HSV-1 infected corneas. Our results suggest that manipulating CXCR4 signaling in HSV-1 infected corneas can have therapeutic implications in reducing the severity of herpes stromal keratitis (HSK).

Methods

Mice

Eight to twelve-week-old female C57BL/6J mice used in our experiments were procured from the Jackson Laboratory (Bar Harbor, ME). All mice were housed in the Association for Assessment and Accreditation of Laboratory Animal Care (AAALAC)- accredited pathogen-free animal facility at Wayne State University School of Medicine (WSUSOM). All manipulations after corneal HSV-1 infection were performed in a type II biosafety cabinet. All experimental procedures were in complete agreement with the Association for Research in Vision and Ophthalmology resolution on the use of animals in research. All experimental procedures undertaken were in accordance with the Institutional Animal Care and Use Committee of Wayne State University.

Corneal HSV-1 infection

HSV-1 McKrae strain was used in the current study. Prior to corneal HSV-1 infection, C57BL6/J mice were given an intraperitoneal (i.p.) administration of ketamine HCl (100 mg/mL) and xylazine HCl (20 mg/mL) solution, which was prepared in 1X DPBS. The total volume administered was 200-220 µl/mouse. Once anesthetized, mild scarification of the corneal epithelium was carried out with 27G ½ inch needle (BD, cat#305109) followed by topical application of 1000 plaque forming units of HSV-1 prepared in 1X DPBS. Only one eye was infected, and infected mice were housed in disposable micro isolator cages.

Real-time-quantitative PCR (RT-qPCR) assay

Total RNA was purified from individual whole cornea dissected from naive and infected eyes using RNeasy® Micro Kit (Qiagen). Briefly, the individual corneas were kept in the 450 µl of RLT buffer (provided in the Micro Kit) and the tissue was disrupted in TissueLyser II. cDNA was prepared using RT^2 First Strand Kit (Qiagen) by reverse transcribing total RNA as per the manufacturer's instruction. CFX Connect Real-Time System (Bio-Rad Laboratories) was used to carry out the RT-qPCR assay. Data were analyzed as fold change in mRNA expression after normalization with housekeeping ß-actin gene using the $2^{-\Delta\Delta CT}$ method. The primers used in the study were procured from Qiagen (RT^2 qPCR Primer Assays). Mouse CXCR4, Gene Globe ID-PPM03149E-200 and Mouse CXCL12, Gene Globe ID- PPM02965E-200.

Immunofluorescence staining

Immunofluorescence to detect CXCR4 and CXCL12 protein was carried out on 8-µm-thick frozen corneal sections. The corneal sections were prepared from the eye with HSK lesion at 16-day post-infection (p.i.). Frozen corneal sections collected on glass slides were fixed in 2% paraformaldehyde for 30 minutes at room temperature. Sections were washed three times in 1X PBS followed by blocking with blocking buffer (1X PBS + 3% BSA + 0.3% Triton-X-100) for 2 hours at room temperature. After 2 hours, sections were incubated with primary unconjugated anti-CXCR4 (R&D systems; MAB21651) or anti-CXCL12 (R&D systems; MAB350-100) antibody overnight at 4°C. The next day, slides were washed three times with 1X PBS + 0.3% Triton-X-100 solution and then incubated at room temperature

for 2 hours with Alexa Fluor 488 conjugated secondary antibody. Next, the slides were washed three times with 1X PBS + 0.3% Triton-X-100 solution and later mounted with DAPI containing mounting medium (Vector Laboratories, CA). Images were acquired using a Leica Confocal Scanner SP8 confocal microscope. Antibody dilutions were made in dilution buffer (1X PBS + 1% BSA + 0.3% Triton-X-100).

Separation of corneal epithelium from stroma

The procedure for the separation of intact corneal epithelial sheet from the underlying corneal stroma was same for uninfected and HSV-1 infected corneas. For flow cytometry, eye balls were enucleated and incubated overnight in 15mg/mL Dispase II enzyme at 4°C. After 16 hours of incubation, the intact corneal epithelium was peeled from the stroma under the stereomicroscope. Next, the corneal stroma was dissected from the eye ball and the remnants of iris were removed from the intact corneal stroma.

Single cell preparation for flow cytometry

Corneal Epithelium—To prepare single cell suspension of the corneal epithelium, individual corneal epithelium sheets removed from uninfected and HSV-1 infected corneas were incubated for 6 minutes in 0.25% Trypsin-EDTA at 37°C in a CO_2 cell culture incubator. To deactivate trypsin, soyabean trypsin inhibitor was added at 2 mg/mL and the live cells in the suspension were counted under phase-contrast microscope using 0.4% trypan-blue solution.

Corneal Stroma—To prepare single cell suspension of the corneal stroma separated from uninfected and HSV-1 infected corneas, individual corneal stroma was incubated in 200 μl of RPMI medium with 20 μl of 2.5 mg/mL Liberase TL reconstituted in RPMI medium only. The stromas were incubated in this solution on a disruptor genie stirrer at 1500 rpm for 30 minutes at 37°C. At the end of the incubation period, 1 mL of complete RPMI medium was added to stop the enzymatic activity of Liberase. The samples were triturated using a 3 mL syringe plunger and passed through a 70 μm cell strainer, followed by pelleting down the cells at 1000 rpm for 10 minutes in a refrigerated centrifuge. Single-cell suspension from individual corneal stroma was plated in a 96-well U-bottom plate for flow cytometry studies.

Flow Cytometry to characterize CXCR4-expressing cells in the corneal epithelium and stroma

The single-cell suspension obtained from individual corneal epithelium and stroma was plated in 96-well U-bottom plate. For cell surface staining, the cells were washed with PBS followed by staining to discriminate live and dead cells using live/dead fixable aqua dead cell stain kit (Invitrogen; L34957). After live/dead staining, the cells were washed with FACS buffer followed by blocking of Fc receptors and incubation with fluorochrome-conjugated antibodies. The following fluorochrome-conjugated antibodies were used for cell surface staining: Alexa-647 anti-CD184 (CXCR4), PE-anti-CD207 (langerin), APC-Cy7 anti-CD326, BV605 anti-CD45, FITC-anti-CD11b, BV421- anti-IA^b, Alexa 700 anti-LY6G, PE-CY7 anti-CD11C, Percp-Cy5.5 anti-F4/80, PE-CF594 anti-CD39. These antibodies were purchased either from BioLegend or BD Biosciences, San Diego, CA. At the end of cell surface staining, the cells were fixed overnight in 2% paraformaldehyde (PFA). Samples

were acquired using LSRFortessa (BD Biosciences) flow cytometer, and the data were analyzed using FlowJo version 10.7.1 software (Ashland, OR, USA).

EdU (5-ethynyl-2-deoxyuridine) cell proliferation assay

EdU staining was carried out using Click-iT™ EdU Pacific blue flow cytometry cell proliferation assay kit (Thermo fisher Scientific; C10418), as per the manufacturer's instruction. Briefly, uninfected and HSV-1 infected C57BL/6J mice received an i.p. injection of 200 μl of EdU (1mg/mL) in 1xPBS. After 18 hours, the mice were euthanized and eye balls were enucleated to separate the epithelium from uninfected and virus-infected corneas. Single cell suspension of the corneal epithelium was prepared for cell surface staining as described above. After cell surface staining, the cells were fixed in Click-iT fixative (component D) for 15 minutes at room temperature followed by the washing in FACS buffer. Next, the cells were permeabilized in 1X Click-iT saponin based permeabilization and wash reagent (component E) for 15 minutes at room temperature in dark. During the incubation period, the master mix solution of click-iT reaction was prepared and the master mix cocktail was added to cells for 30 minutes at room temperature. At the end of incubation period, cells were washed two times in click-iT permeabilization buffer. Finally, the cells were fixed in 2% paraformaldehyde and the samples were acquired using LSRFortessa flow cytometer.

Statistical analysis

All statistical analysis was done using GraphPad Prism 9 (San Diego, CA). Significance was determined by nonparametric Mann–Whitney U test. One-way or Two-way ANOVA was used to determine statistically significant differences when comparing the results of more than two independent groups.

Results

LCs are the prominent CXCR4 expressing cells in uninfected corneal epithelium

We recently published an approach to perform flow cytometry on the individual corneal epithelium (CE) and corneal stroma (CS) separated from uninfected and HSV-1-infected corneas [18]. The single-cell suspension of individual CE separated from uninfected mouse corneas was used for flow cytometry to enumerate and characterize CXCR4-expressing cells (Fig. 1A). The parent gating strategies employed to remove debris, dead cells, and doublets from the single-cell suspension of the CE are shown in Fig. 1B. Our flow cytometry results showed CXCR4-expressing cells in the separated epithelium of uninfected corneas (Fig. 1C). The CE is the home of CD11c+ dendritic cells including CD207+LCs [4]. Therefore, we ascertained whether CXCR4-expressing cells in the CE of naïve corneas bear the phenotype of LCs. The single cell suspension of CE was stained for the markers of LCs. Our results showed that an average of 57% of CXCR4+ cells in the uninfected CE expressed CD207 (langerin) molecule (Fig. 1C and 1D). On the other hand, almost all CD207-expressing cells in naïve CE expressed CXCR4 molecule (Supplementary Figure 1). The CD207-expressing cells in uninfected CE can be LCs; the latter is known to express the CD11c molecule [19, 20]. Therefore, CD11c expression was measured on CD207+CXCR4+ cells. Our data showed $CD11c^{hi}$ and $CD11c^{lo}$ expressing CD207+CXCR4+ LCs subsets

in the uninfected CE. These two subsets of CXCR4-expressing LCs expressed a similar level of CD39, a dominant LC-associated membrane-bound ATPase. However, $CD11c^{hi}$ LCs expressed a significantly higher level of MHC class II and CD326 than $CD11c^{lo}$ LCs (Fig. 1C and 1E). On the other hand, non-langerin (CD207-ve) CXCR4+ cells in the CE of naïve mice exhibited the phenotype of APCs, as they expressed CD45 and MHC class II molecules (Fig. 1C). Together, our results showed the presence of CXCR4-expressing resident APCs, including LCs, in the CE of uninfected mouse corneas.

Macrophages are the prominent CXCR4 expressing cells in the uninfected CS

CS is known to harbor the CD11b expressing macrophages [3], and the macrophages can express CXCR4 protein [21]. Therefore, we next ascertained whether CXCR4-expressing cells are present in the CS of naïve mouse cornea. The CS was separated from uninfected mouse cornea (Fig. 2A). The gating strategies employed to remove debris, dead cells, and doublets from the single-cell suspension of the individual corneal stroma are shown in Fig. 2B. Our flow cytometry results showed the presence of CXCR4-expressing cells in the CS of naïve mice (Fig. 2C). However, in contrast to CE, almost all CXCR4-expressing cells in the CS of uninfected eyes were CD207-ve but expressed leukocytic marker CD45. Furthermore, these CXCR4+CD207-ve leukocytes expressed CD11b, F4/80, and MHC class II molecules documenting the phenotype of stromal resident macrophages (Fig. 2D). Taken together, our results showed that LCs are the predominant CXCR4-expressing cells in the CE. In contrast, the macrophages are the prominent CXCR4-expressing cells in the CS of uninfected C57Bl/6J corneas.

An increased level of CXCR4 and CXCL12 mRNA transcripts in HSK corneas

We recently reported the occurrence of hypoxia in HSV-1-infected corneas [22]. Hypoxia is known to upregulate the expression of CXCR4 and its ligand CXCL12 [23, 24]. Therefore, we assessed the mRNA expression profile of CXCR4 and its ligand CXCL12 between uninfected and HSV-1 infected corneas. Our results showed that in comparison to uninfected corneas, HSV-1 infected corneas showed an average of 9-, 23-, 26-, and a 30-fold increase in CXCR4 mRNA levels at 4-, 9-, 12-, and 16-day p.i., respectively (Fig. 3A). In contrast, a moderate but non-significant increase in CXCL12 mRNA level was noted in HSV-1 infected corneas at 4- and 9-day p.i. However, at 12-days p.i., during the progression of HSK, an about 3-fold increase in CXCL12 mRNA level was seen in infected than uninfected corneas. At 16 days p.i., the corneas with HSK showed an average 5-fold increase in CXCL12 mRNA than uninfected corneas (Fig. 3C). We chose these time points to reflect the four different stages of HSK development (Fig. 3B). The 4-day p.i. is considered a pre-clinical period during which infectious virus is present. However, the corneal opacity and hemangiogenesis are not seen. The progression of corneal opacity, epithelial defect, and hemangiogenesis is evident at 9- and 12- days p.i. The full-blown HSK with severe corneal opacity, hemangiogenesis, and epithelial defect is noticed at 16 days p.i. (Fig. 3B). Our results also showed a significantly increased level of CXCR4 in the separated epithelium and stroma of HSV-1 infected corneas at 4- and 16-day p.i. (Fig. 3D). On the other hand, a significantly increased level of CXCL12 was seen in the separated epithelium and stroma of infected than uninfected corneas during clinical (16-day p.i.) but not pre-clinical (4-day p.i.)

time-period (Fig. 3E). Together, our results showed a significantly increased mRNA level of CXCR4 and CXCL12 in HSK than naïve corneas.

Immunofluorescence of CXCR4 and CXCL12 protein in HSK corneas

Next, we ascertained CXCR4 and CXCL12 protein localization in HSK corneas. The immunofluorescence staining for CXCR4 and CXCL12 protein was carried out in the frozen sections of HSK corneas at 16 days p.i. (Fig. 4A). As is shown in Fig. 4B, a prominent CXCL12 protein staining was evident in the cross-sections of the stromal blood vessels. No prominent CXCL12 staining was seen in the CE. Our results also showed intense CXCR4 staining in the epithelium and stroma of HSK corneas (Fig. 4B). In the stroma, CXCR4 staining was displayed in the cross-sections of stromal blood vessels of HSK corneas. Additionally, membrane-bound CXCR4 staining was also seen on cells in the anterior stroma and basal layer of the corneal epithelium of the HSK cornea. Isotype controls did not show non-specific staining in HSK corneas.

Corneal HSV-1 infection causes a transient increase in the number of CXCR4-expressing LCs in the CE of infected corneas

Next, we measured the outcome of corneal HSV-1 infection on CXCR4+ cells in the CE of HSV-1 infected corneas at 4-, 9-, and 16-day p.i. Single-cell suspension prepared from the individual CE of infected corneas was used for flow cytometry. Our results showed that compared to the uninfected CE, the HSV-1 infected CE displayed an increased frequency and number of CXCR4+ cells at 4 days p.i. (Fig. 5A). However, by 9 days p.i., the frequency and number of CXCR4+ cells declined to the counts observed in the naïve CE. Since most CXCR4+ cells in uninfected CE exhibit the LCs phenotype (Figure 1), we next determined whether the transient increase in CXCR4+ cells in HSV-1 infected cornea is the outcome of an increase in CD207+CXCR4+ LCs. Our results showed that compared to naïve CE, the HSV-1 infected CE exhibited increased CD207+CXCR4+ LCs at 4 days p.i. However, by 9 days p.i., CD207+CXCR4+ LCs number in the CE declined to the counts seen in the naïve CE (Fig. 5B). To test whether an increased number of CD207+CXCR4+LCs at 4 days p.i. in the epithelium resulted from their proliferation, we performed an *in vivo* EdU labeling of proliferating cells. Our results showed an approximately 6-fold increase in the frequency and the absolute number of EdU+CD207+ LCs in the CE of HSV-1 infected corneas at 4-day p.i. than uninfected corneas (Figure 5C).

Neutrophils and vascular endothelial cells are the prominent CXCR4 expressing cells in the stroma of HSK corneas

CXCR4 expression has been reported on neutrophils after extravasation into inflamed lung tissue [25]. Similarly, CXCR4 signaling is reported to promote hemangiogenesis in tumor models [26]. Therefore, we next ascertained whether infiltrated neutrophils and newly formed blood vessels in HSK corneas express membrane-bound CXCR4 molecule. The single-cell suspension of the individual CS separated from the epithelium of HSK corneas was used to perform the flow cytometry assay. The gating strategies employed to exclude debris and dead cells to obtain the singlets for analysis are shown in Fig. 6B. Our results showed that more than 60% of CD45+ leukocytes expressed membrane-bound CXCR4 molecule in the CS of HSK cornea. Among CXCR4-expressing leukocytes, more than 80%

were CD11b+ cells and exhibited the myeloid cell phenotype. Furthermore, among CXCR4-expressing myeloid cells, our results showed 84.8% neutrophils, 8.7% monocytes, and 3.4% Ly6g-ve Ly6C-ve cells. In addition to myeloid cells, approximately 5% of CXCR4+CD45+ cells were TCR-beta+, showing the T cell phenotype. Although CD4 T cells are the primary T cell subset in HSK corneas [27], our results showed that only 35% of CXCR4+ T cells were CD4 T cells (Fig. 6C). On the other hand, most CXCR4− veCD45+ leukocytes were CD4 T cells (Fig. 6C). Collectively, these results showed that neutrophils but not CD4 T cells are the prominent CXCR4 expressing immune cells in HSK cornea.

Stromal neovascularization is the hallmark of HSK and is clearly evident in the separated stroma of HSK corneas at 16-day p.i. (Fig. 6A). CD31-expressing vascular endothelial cells are previously reported to quantify corneal angiogenesis in the mouse model of HSK [28]. Therefore, we next ascertained whether CD31+ cells in the stroma of HSK corneas expressed CXCR4 molecule. Our results showed a distinct population of CD31+CD45-ve cells in the corneal stroma (Fig. 6D). Depending upon the extent of hemangiogenesis in HSK corneas, the frequency of these cells ranges from 0.30 to 0.83% of CD45-ve cells. Furthermore, an average of 45% of CD31+CD45-ve cells expressed CXCR4 protein in the stroma of HSK corneas at 16-day p.i. (Fig. 6D). Together, these results showed a significant fraction of vascular endothelial cells expressing CXCR4 in HSK lesions.

Discussion

Chemokine receptor-mediated signaling can be essential in homing stem cells, progenitors, and immune cells. CXCR4 signaling is reported to control the location of dendritic cells under a steady state and in inflammation [29]. Additionally, it has been shown that CXCR4 mediates conventional CD11c+ dendritic cell recruitment into the suture-induced inflamed murine cornea [16]. The epithelium of murine and human corneas is populated with CD207+ LCs [30-32]. Our results showed that most CXCR4-expressing cells in the uninfected epithelium are corneal resident LCs. Our data also suggest two subsets of corneal resident LCs based on CD11c expression level. $CD11c^{hi}$ and $CD11c^{lo}$ subsets expressed a similar level of CD39, a dominant LCs-associated ectonucleotidase [33]. In contrast, the $CD11c^{hi}$ subset expressed a significantly higher level of CD326 than the $CD11c^{lo}$ subset. CD326 expression on epidermal LCs promotes their motility [34]. Therefore, the $CD11c^{hi}$ subset of corneal-resident LCs may be more mobile than the $CD11c^{lo}$ LC subset. LCs are documented to play an important role in the development of HSK in murine corneas [35, 36]. However, the underlying mechanisms still need to be clarified. Our results showed that LCs proliferate in response to corneal HSV-1 infection, increasing their numbers in the epithelium at 4-day p.i. However, by 9-days p.i., the numbers have reduced to the counts seen in the naïve epithelium. Since LCs are reported to migrate to the site of corneal HSV-1 infection [4], CXCR4+ LCs, after acquiring the viral antigens, may migrate from CE to CS of HSK-developing corneas. In support, the chemotactic signal (CXCL12) to attract CXCR4+LCs is present in the CS of HSK corneas. In the skin, LCs can migrate from the epidermis to the dermis and are involved in antigen presentation to T cells [37, 38]. Similarly, in the CS, the LCs can present viral antigens to differentiated CD4 T cells and potentiate their effector function. Thus, impeding the migration of LCs from the CE to CS

of HSV-1 infected corneas may reduce the severity of HSK. Our ongoing experiments are testing this hypothesis.

In addition to CE, we also detected CXCR4-expressing cells in the stroma of the uninfected cornea. Our results showed that most CXCR4-expressing cells exhibited the phenotype of stromal macrophages in the uninfected cornea. A recent study showed that CXCR4 expression could distinguish monocyte-derived macrophages from tissue-resident macrophages in the brain tissues [39]. The tissue-resident macrophages originate from yolk-sac but get supplemented by bone-marrow derived monocytes after birth. Our results may distinguish monocyte-derived macrophages from yolk-sac derived macrophages in the corneal stroma. Furthermore, corneal stromal macrophages have also been shown to interact with stromal nerve trunks [40]. The possible involvement of CXCR4-CXCL12 signaling in these interactions cannot be ruled out, as peripheral nerves are reported to produce CXCL12 chemokine [41].

It is well reported that CXCR4 and CXCL12 expression gets upregulated under hypoxic conditions [23, 42, 43]. We recently reported the occurrence of hypoxia in progressing HSK lesions [22]. Accordingly, the results shown in this study demonstrated an upregulation of CXCR4 and CXCL12 in HSK corneas. The CXCR4-CXCL12 axis promotes hemangiogenesis in proliferative diabetic retinopathy [44]. CXCL12 secreted from vascular endothelial cells can act directly on CXCR4 expressing blood vessels and promote their vascular growth. In support, our immunofluorescence data showed CXCL12 staining in the cross-sections of newly developed blood vessels in the HSK cornea. Furthermore, a significant proportion of CD31+ vascular endothelial cells in the stroma of HSK corneas expressed CXCR4. These results suggest the possible involvement of CXCR4-CXCL12 interactions in promoting hemangiogenesis in HSK.

Neutrophils are the major immune cell type in the HSK cornea, and CXCR2-mediated signaling plays a pivotal role in attracting neutrophils in HSK lesions [45, 46]. However, after extravasation, the surface expression of CXCR4 is increased on neutrophils [25]. Our results also showed that most of the CXCR4 expressing leukocytes in the stroma of HSK corneas were neutrophils. Since CXCR4-CXCL12 signaling is involved in homing different cell types, these interactions may promote the retention of neutrophils in the HSK cornea. In fact, the use of CXCR4 antagonist AMD3100 has been reported to promote the reverse migration of neutrophils from the site of inflammation in a zebrafish model [47]. The ongoing experiments test whether localized blocking of the CXCR4-CXCL12 axis promotes the reverse migration of neutrophils from HSK developing corneas.

Collectively, our results showed CXCR4 expression on resident APCs in the uninfected cornea and infiltrating neutrophils and newly formed blood vessels in the HSK cornea, suggesting a pleiotropic effect of CXCR4 signaling in HSK. Considering the effectiveness of targeting chemokine receptors in the clinic, CXCR4 can serve as a potential therapeutic target in HSK. The ongoing experiments are testing this concept.

Supplementary Material

Refer to Web version on PubMed Central for supplementary material.

Disclosure:

The authors have no financial conflict of interest. The work was supported by National Institutes of Health grants R01EY030129 and R01EY029690 awarded to Dr. Susmit Suvas.

Supported by National Eye Institute Grant R01EY029690 and R01EY030129 awarded to Dr. Suvas, Research to Prevent Blindness (unrestricted grant to Kresge Eye Institute) and P30EY04068 awarded to Linda Hazlett.

References:

[1]. Hamrah P, Huq SO, Liu Y, Zhang Q, Dana MR. Corneal immunity is mediated by heterogeneous population of antigen-presenting cells. J Leukoc Biol. 2003;74:172–8. [PubMed: 12885933]

[2]. Knickelbein JE, Watkins SC, McMenamin PG, Hendricks RL. Stratification of Antigen-presenting Cells within the Normal Cornea. Ophthalmol Eye Dis. 2009;1:45–54. [PubMed: 20431695]

[3]. Brissette-Storkus CS, Reynolds SM, Lepisto AJ, Hendricks RL. Identification of a novel macrophage population in the normal mouse corneal stroma. Invest Ophthalmol Vis Sci. 2002;43:2264–71. [PubMed: 12091426]

[4]. Knickelbein JE, Buela KA, Hendricks RL. Antigen-presenting cells are stratified within normal human corneas and are rapidly mobilized during ex vivo viral infection. Invest Ophthalmol Vis Sci. 2014;55:1118–23. [PubMed: 24508792]

[5]. Hughes CE, Nibbs RJB. A guide to chemokines and their receptors. FEBS J. 2018;285:2944–71. [PubMed: 29637711]

[6]. Ono SJ, Nakamura T, Miyazaki D, Ohbayashi M, Dawson M, Toda M. Chemokines: roles in leukocyte development, trafficking, and effector function. J Allergy Clin Immunol. 2003;111:1185–99; quiz 200. [PubMed: 12789214]

[7]. Tang P, Wang JM. Chemokines: the past, the present and the future. Cell Mol Immunol. 2018;15:295–8. [PubMed: 29578534]

[8]. Griffith JW, Sokol CL, Luster AD. Chemokines and chemokine receptors: positioning cells for host defense and immunity. Annu Rev Immunol. 2014;32:659–702. [PubMed: 24655300]

[9]. Zlotnik A, Burkhardt AM, Homey B. Homeostatic chemokine receptors and organ-specific metastasis. Nat Rev Immunol. 2011;11:597–606. [PubMed: 21866172]

[10]. Pozzobon T, Goldoni G, Viola A, Molon B. CXCR4 signaling in health and disease. Immunol Lett. 2016;177:6–15. [PubMed: 27363619]

[11]. Jacobson O, Weiss ID. CXCR4 chemokine receptor overview: biology, pathology and applications in imaging and therapy. Theranostics. 2013;3:1–2. [PubMed: 23382779]

[12]. Loetscher M, Geiser T, O'Reilly T, Zwahlen R, Baggiolini M, Moser B. Cloning of a human seven-transmembrane domain receptor, LESTR, that is highly expressed in leukocytes. J Biol Chem. 1994;269:232–7. [PubMed: 8276799]

[13]. Shirozu M, Nakano T, Inazawa J, Tashiro K, Tada H, Shinohara T, et al. Structure and chromosomal localization of the human stromal cell-derived factor 1 (SDF1) gene. Genomics. 1995;28:495–500. [PubMed: 7490086]

[14]. Martin C, Burdon PC, Bridger G, Gutierrez-Ramos JC, Williams TJ, Rankin SM. Chemokines acting via CXCR2 and CXCR4 control the release of neutrophils from the bone marrow and their return following senescence. Immunity. 2003;19:583–93. [PubMed: 14563322]

[15]. Goedhart M, Gessel S, van der Voort R, Slot E, Lucas B, Gielen E, et al. CXCR4, but not CXCR3, drives CD8(+) T-cell entry into and migration through the murine bone marrow. Eur J Immunol. 2019;49:576–89. [PubMed: 30707456]

[16]. Lopez MJ, Seyed-Razavi Y, Jamali A, Harris DL, Hamrah P. The Chemokine Receptor CXCR4 Mediates Recruitment of CD11c+ Conventional Dendritic Cells Into the Inflamed Murine Cornea. Invest Ophthalmol Vis Sci. 2018;59:5671–81. [PubMed: 30489627]

[17]. Du LL, Liu P. CXCL12/CXCR4 axis regulates neovascularization and lymphangiogenesis in sutured corneas in mice. Mol Med Rep. 2016;13:4987–94. [PubMed: 27121088]

[18]. Setia M, Suvas PK, Suvas S. Flow cytometry protocol to quantify immune cells in the separated epithelium and stroma of herpes simplex virus-1-infected mouse cornea. STAR Protocols. 2023;4:102056. [PubMed: 36790766]

[19]. Wolff K. The fine structure of the Langerhans cell granule. J Cell Biol. 1967;35:468–73. [PubMed: 6055996]

[20]. Valladeau J, Ravel O, Dezutter-Dambuyant C, Moore K, Kleijmeer M, Liu Y, et al. Langerin, a novel C-type lectin specific to Langerhans cells, is an endocytic receptor that induces the formation of Birbeck granules. Immunity. 2000;12:71–81. [PubMed: 10661407]

[21]. Lee C, Liu QH, Tomkowicz B, Yi Y, Freedman BD, Collman RG. Macrophage activation through CCR5- and CXCR4-mediated gp120-elicited signaling pathways. J Leukoc Biol. 2003;74:676–82. [PubMed: 12960231]

[22]. Rao P, Suvas S. Development of Inflammatory Hypoxia and Prevalence of Glycolytic Metabolism in Progressing Herpes Stromal Keratitis Lesions. J Immunol. 2019;202:514–26. [PubMed: 30530484]

[23]. Schioppa T, Uranchimeg B, Saccani A, Biswas SK, Doni A, Rapisarda A, et al. Regulation of the chemokine receptor CXCR4 by hypoxia. J Exp Med. 2003;198:1391–402. [PubMed: 14597738]

[24]. Santiago B, Calonge E, Del Rey MJ, Gutierrez-Canas I, Izquierdo E, Usategui A, et al. CXCL12 gene expression is upregulated by hypoxia and growth arrest but not by inflammatory cytokines in rheumatoid synovial fibroblasts. Cytokine. 2011;53:184–90. [PubMed: 20609598]

[25]. Yamada M, Kubo H, Kobayashi S, Ishizawa K, He M, Suzuki T, et al. The increase in surface CXCR4 expression on lung extravascular neutrophils and its effects on neutrophils during endotoxin-induced lung injury. Cell Mol Immunol. 2011;8:305–14. [PubMed: 21460863]

[26]. Liang Z, Brooks J, Willard M, Liang K, Yoon Y, Kang S, et al. CXCR4/CXCL12 axis promotes VEGF-mediated tumor angiogenesis through Akt signaling pathway. Biochem Biophys Res Commun. 2007;359:716–22. [PubMed: 17559806]

[27]. Doymaz MZ, Rouse BT. Herpetic stromal keratitis: an immunopathologic disease mediated by CD4+ T lymphocytes. Invest Ophthalmol Vis Sci. 1992;33:2165–73. [PubMed: 1351475]

[28]. Biswas PS, Banerjee K, Kim B, Smith J, Rouse BT. A novel flow cytometry based assay for quantification of corneal angiogenesis in the mouse model of herpetic stromal keratitis. Exp Eye Res. 2005;80:73–81. [PubMed: 15652528]

[29]. Gallego C, Vetillard M, Calmette J, Roriz M, Marin-Esteban V, Evrard M, et al. CXCR4 signaling controls dendritic cell location and activation at steady state and in inflammation. Blood. 2021;137:2770–84. [PubMed: 33512478]

[30]. Chandler JW, Cummings M, Gillette TE. Presence of Langerhans cells in the central corneas of normal human infants. Invest Ophthalmol Vis Sci. 1985;26:113–6. [PubMed: 3967954]

[31]. Williamson JS, DiMarco S, Streilein JW. Immunobiology of Langerhans cells on the ocular surface. I. Langerhans cells within the central cornea interfere with induction of anterior chamber associated immune deviation. Invest Ophthalmol Vis Sci. 1987;28:1527–32. [PubMed: 3623837]

[32]. Hattori T, Chauhan SK, Lee H, Ueno H, Dana R, Kaplan DH, et al. Characterization of Langerin-expressing dendritic cell subsets in the normal cornea. Invest Ophthalmol Vis Sci. 2011;52:4598–604. [PubMed: 21482644]

[33]. Mizumoto N, Kumamoto T, Robson SC, Sevigny J, Matsue H, Enjyoji K, et al. CD39 is the dominant Langerhans cell-associated ecto-NTPDase: modulatory roles in inflammation and immune responsiveness. Nat Med. 2002;8:358–65. [PubMed: 11927941]

[34]. Gaiser MR, Lammermann T, Feng X, Igyarto BZ, Kaplan DH, Tessarollo L, et al. Cancer-associated epithelial cell adhesion molecule (EpCAM; CD326) enables epidermal Langerhans cell motility and migration in vivo. Proc Natl Acad Sci U S A. 2012;109:E889–97. [PubMed: 22411813]

[35]. Jager MJ, Bradley D, Atherton S, Streilein JW. Presence of Langerhans cells in the central cornea linked to the development of ocular herpes in mice. Exp Eye Res. 1992;54:835–41. [PubMed: 1325920]

[36]. Hendricks RL, Janowicz M, Tumpey TM. Critical role of corneal Langerhans cells in the CD4- but not CD8-mediated immunopathology in herpes simplex virus-1-infected mouse corneas. J Immunol. 1992;148:2522–9. [PubMed: 1313845]

[37]. Villablanca EJ, Mora JR. A two-step model for Langerhans cell migration to skin-draining LN. Eur J Immunol. 2008;38:2975–80. [PubMed: 18991275]

[38]. Stoitzner P, Tripp CH, Eberhart A, Price KM, Jung JY, Bursch L, et al. Langerhans cells cross-present antigen derived from skin. Proc Natl Acad Sci U S A. 2006;103:7783–8. [PubMed: 16672373]

[39]. Werner Y, Mass E, Ashok Kumar P, Ulas T, Handler K, Horne A, et al. Cxcr4 distinguishes HSC-derived monocytes from microglia and reveals monocyte immune responses to experimental stroke. Nat Neurosci. 2020;23:351–62. [PubMed: 32042176]

[40]. Seyed-Razavi Y, Chinnery HR, McMenamin PG. A novel association between resident tissue macrophages and nerves in the peripheral stroma of the murine cornea. Invest Ophthalmol Vis Sci. 2014;55:1313–20. [PubMed: 24458151]

[41]. Li W, Kohara H, Uchida Y, James JM, Soneji K, Cronshaw DG, et al. Peripheral nerve-derived CXCL12 and VEGF-A regulate the patterning of arterial vessel branching in developing limb skin. Dev Cell. 2013;24:359–71. [PubMed: 23395391]

[42]. Strickland J, Garrison D, Copple BL. Hypoxia upregulates Cxcl12 in hepatocytes by a complex mechanism involving hypoxia-inducible factors and transforming growth factor-beta. Cytokine. 2020;127:154986. [PubMed: 31951966]

[43]. Ceradini DJ, Kulkarni AR, Callaghan MJ, Tepper OM, Bastidas N, Kleinman ME, et al. Progenitor cell trafficking is regulated by hypoxic gradients through HIF-1 induction of SDF-1. Nat Med. 2004;10:858–64. [PubMed: 15235597]

[44]. Butler JM, Guthrie SM, Koc M, Afzal A, Caballero S, Brooks HL, et al. SDF-1 is both necessary and sufficient to promote proliferative retinopathy. J Clin Invest. 2005;115:86–93. [PubMed: 15630447]

[45]. Thomas J, Gangappa S, Kanangat S, Rouse BT. On the essential involvement of neutrophils in the immunopathologic disease: herpetic stromal keratitis. J Immunol. 1997;158:1383–91. [PubMed: 9013983]

[46]. Banerjee K, Biswas PS, Kim B, Lee S, Rouse BT. CXCR2−/− mice show enhanced susceptibility to herpetic stromal keratitis: a role for IL-6-induced neovascularization. J Immunol. 2004;172:1237–45. [PubMed: 14707102]

[47]. Isles HM, Herman KD, Robertson AL, Loynes CA, Prince LR, Elks PM, et al. The CXCL12/CXCR4 Signaling Axis Retains Neutrophils at Inflammatory Sites in Zebrafish. Front Immunol. 2019;10:1784. [PubMed: 31417560]

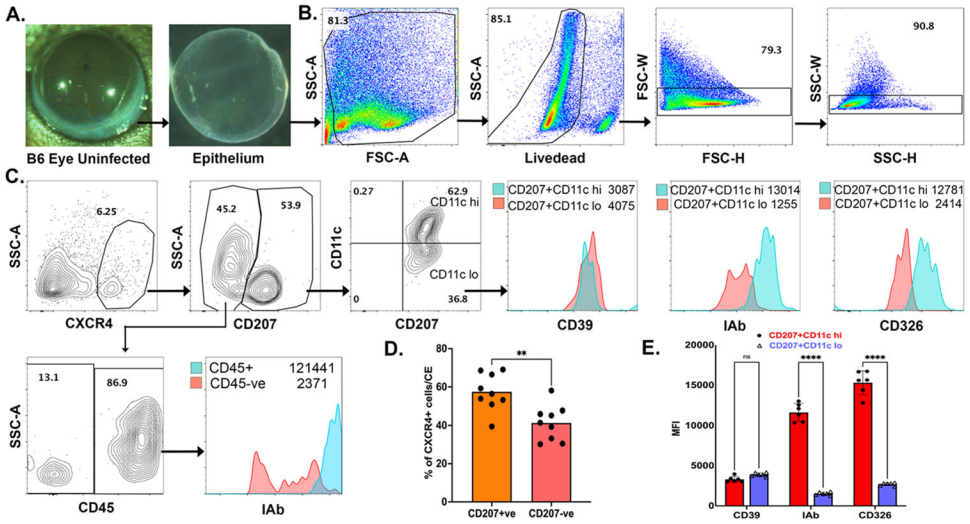

Figure 1. LCs are the prominent CXCR4-expressing cells in the epithelium of uninfected C57BL/6J mouse cornea.

(A) A representative eyeball image from an uninfected mouse and an intact epithelium separated from the uninfected C57BL/6J mouse cornea. **(B)** Representative pseudocolor FACS plots denote the parent gating strategy employed to remove debris, dead cells, and doublets from the single-cell suspension of the uninfected CE used for FACS staining. **(C)** Representative contour FACS plots show the gates employed to determine the frequency of CXCR4 expressing CD207+ and CD207-ve cells in uninfected CE. Histogram overlay shows the expression level of CD39, IA^b, and CD326 surface molecules between $CD11c^{hi}$ and $CD11c^{lo}$ LCs. **(D)** The histogram scatter plot shows the frequency of CXCR4-expressing CD207+ and CXD207-ve cells in individual CE separated from the mouse cornea. Each dot represents an individual CE. Statistical significance was determined using non-parametric Mann-Whitney's test (** $p<0.01$) **(E)** Histogram scatter plot shows the median fluorescence intensity (MFI) of CD39, IA^b, and CD326 on $CD11c^{hi}$ and $CD11c^{lo}$ LCs in individual CE. Two-way ANOVA followed by Sidak multiple comparison analysis was used to determine the statistical significance (ns= non-significant, ****$p<0.0001$)

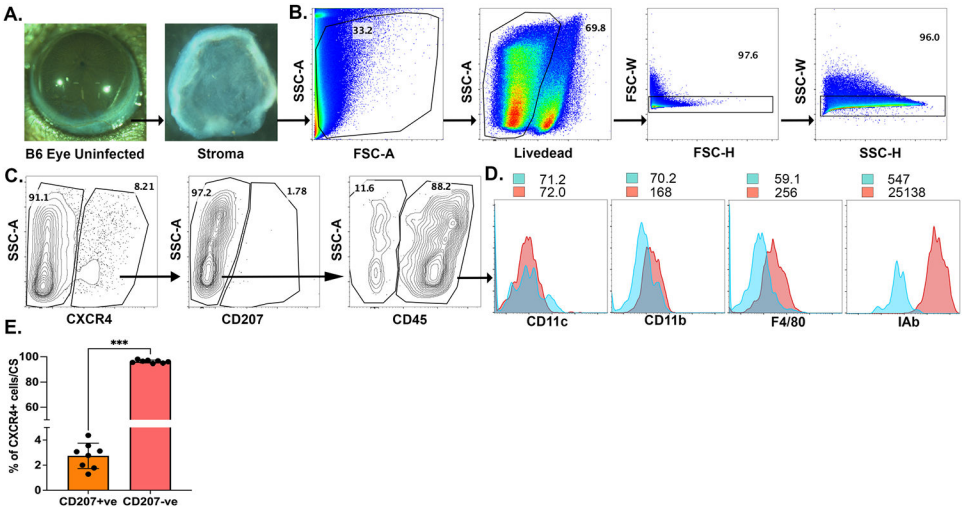

Figure 2. Stromal macrophages are the prominent CXCR4-expressing cells in the uninfected C57BL/6J mouse CS.

(A) Representative image of an uninfected eyeball of the mouse and an intact stroma separated from the uninfected mouse cornea. **(B)** Representative FACS plots denote the gating strategy employed to remove debris, dead cells, and doublets from the single-cell suspension of an uninfected CS. **(C)** Representative contour FACS plots show the gates employed to detect the frequency of cells expressing CXCR4, CD207, and CD45 markers in an individual CS. The arrows point towards the population derived from the parent gate. **(D)** Histogram plot overlays show the median fluorescence intensity (MFI) of Fluorescence minus one (FMO) and CD11c, CD11b, F4/80 and IA^b molecules on CXCR4+CD207-veCD45+ cells in the stroma of the uninfected cornea. **(E)** The Scatter plot shows the frequency of CXCR4-expressing CD207+ and CXD207-ve cells in individual CS separated from the mouse cornea. Each dot represents an individual CS. Statistical significance was determined using non-parametric Mann-Whitney's test (*** $p<0.001$).

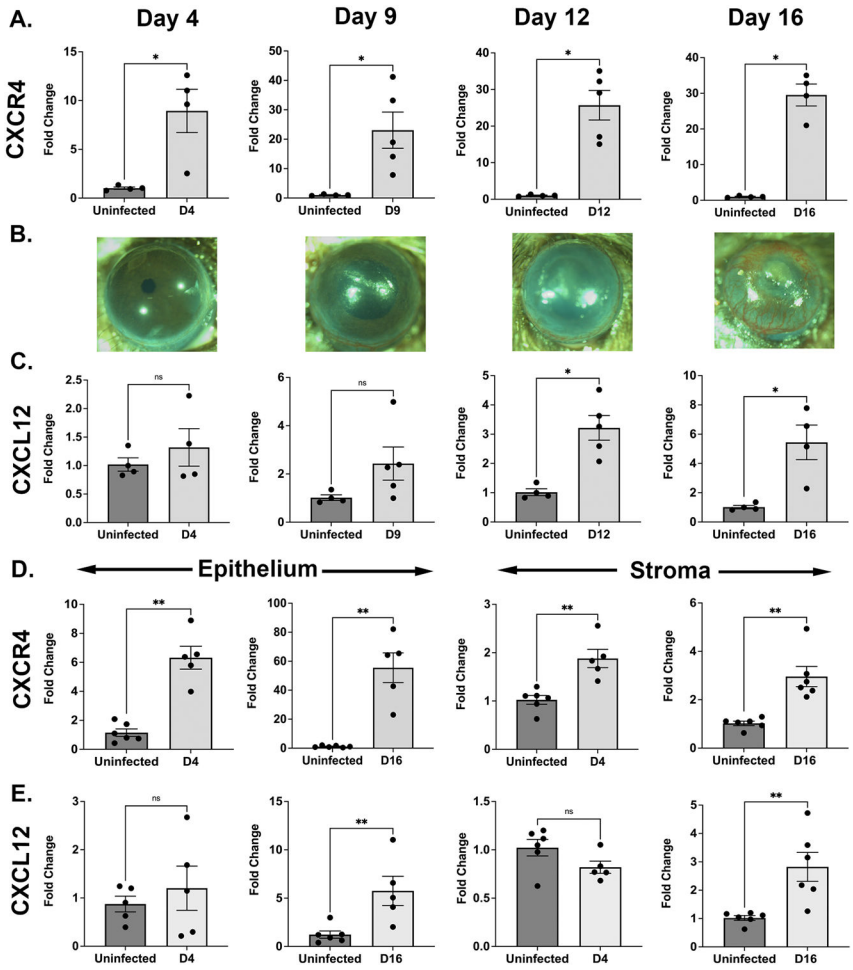

Figure 3. An increased expression of CXCR4 and CXCL12 in the corneas with HSK lesions.

(A) Histogram scatter plots show the fold change in mRNA level of the CXCR4 gene in HSV-1 infected cornea at 4-, 9-, 12-, and 16-day p.i. compared to CXCR4 expression level in uninfected C57BL/6J cornea. **(B)** Representative eye images depict the development of opacity and angiogenesis in HSV-1 infected cornea at 4-, 9-, 12- and 16-day p.i. **(C)** Histogram scatter plots show the fold change in mRNA level of the CXCL12 gene in HSV-1 infected cornea at 4-, 9-, 12-, and 16-day p.i. compared to the expression of CXCL12 in the uninfected mouse cornea. Each dot represents an individual cornea. **(D)** Scatter plots show the fold change in mRNA level of CXCR4 in the separated CE and CS of HSV-1 infected corneas at 4-day and 16-day p.i. than uninfected CE and CS of C57BL/6J mice. **(E)** Bar diagrams denote the fold change in mRNA level of CXCL12 in separated CE and CS of infected corneas at 4-day and 16-day p.i. than uninfected CE and CS of C57BL/6J mice. Non-parametric Mann-Whitney's test was used to calculate the statistical significance (ns = non-significant, and *$p<0.05$ and **$p<0.01$ are considered statistically significant).

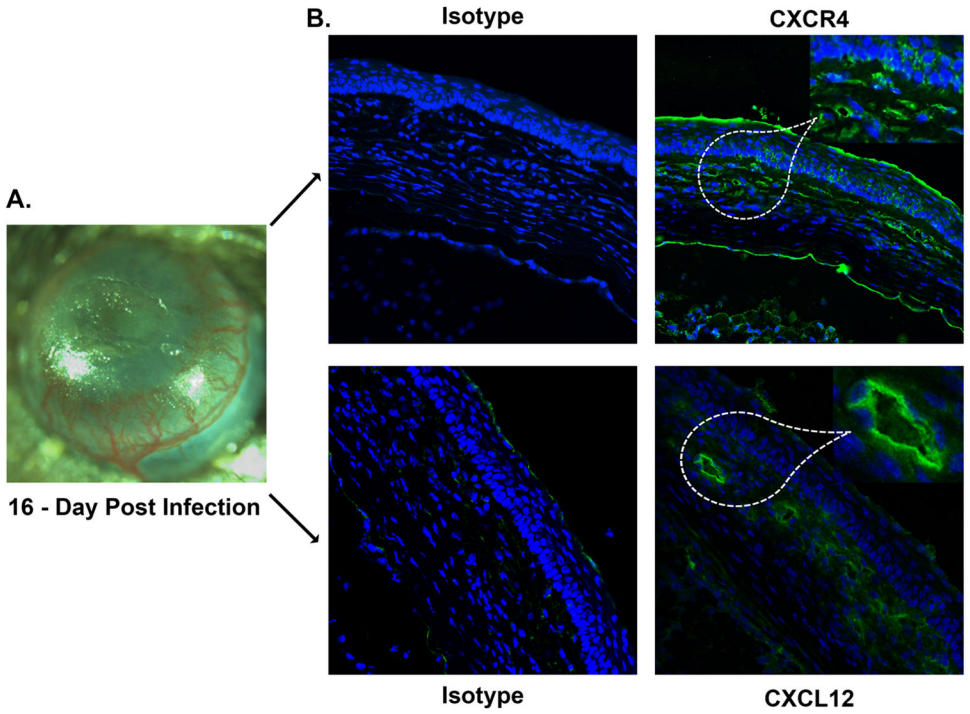

Figure 4. Immunofluorescence staining shows CXCR4 and CXCL12 expressing cells in the frozen sections of HSK cornea at 16-day p.i.

(A) Representative eye image of HSK cornea showing hemangiogenesis and corneal opacity at 16-day p.i. **(B)** Eight-micron frozen sections of HSK cornea were stained (green staining) for either CXCR4 (top panel) or CXCL12 (bottom panel) protein and counterstained with DAPI (blue) for nuclear staining. CXCR4 staining was seen in the epithelium and stroma, while CXCL12 staining was highly localized in the cross-sections of blood vessels in the corneal stroma. The sections were imaged using Leica confocal microscope. Images were acquired at 40X magnification for CXCR4 and 40X +1.7 digital zoom for CXCL12 protein. Inset shows the magnified view of dotted area in the frozen sections of the HSK cornea.

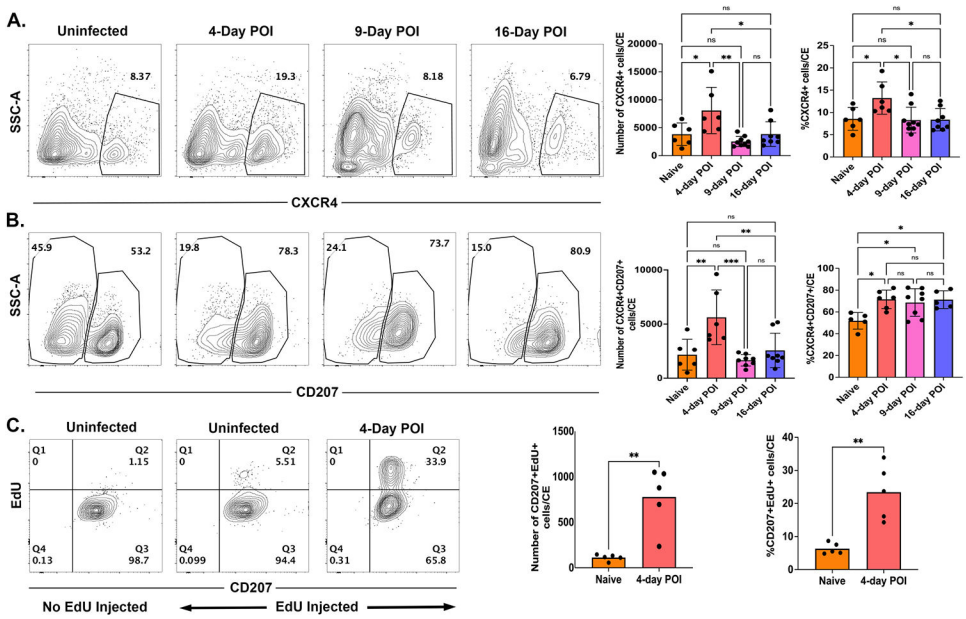

Figure 5. Corneal HSV-1 infection causes a transient increase in CXCR4-expressing LCs in the CE during the lytic phase of viral infection.

(A) Representative FACS plots show the frequency of CXCR4 expressing singlets in uninfected and HSV-1 infected corneas. Scatter plot histograms show a significant increase in the frequency and number of CXCR4-expressing cells at 4-day p.i. **(B)** Representative FACS plots are derived from CXCR4+ cells, and histogram scatter plots show significantly increased frequency and number of CXCR4 expressing CD207+ cells at 4-day p.i. **(C)** Representative contour plots show the frequency of EdU+CD207+ cells in uninfected CE and HSV-1 infected CE at 4-day p.i. Scatter plot histograms show a significant increase in the frequency and number of EdU+CD207+ cells in the CE at 4-day p.i. Ordinary one-way ANOVA or Mann-Whitney test was used to calculate the level of significance. ns=non-significant and *p<0.05, **p<0.01, and ***p<0.001 were considered statistically significant.

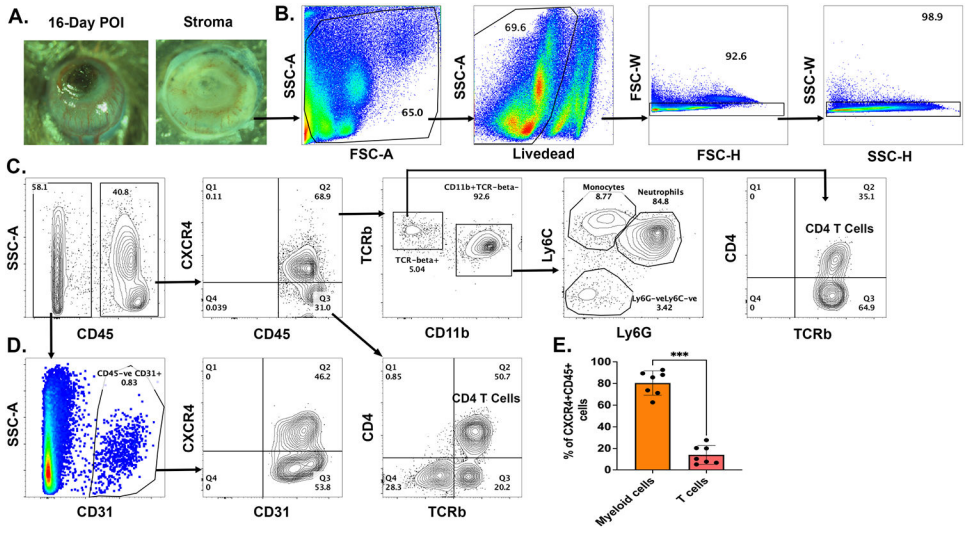

Figure 6. The cell surface expression of CXCR4 in the stroma of HSK corneas is localized on neutrophils and vascular endothelial cells.

(A) Representative eye image showing angiogenesis and opacity in HSK cornea at 16-day post-infection. **(B)** FACS plots denoting the parent gating strategies employed to remove debris, dead cells, and doublets from the single-cell suspension of an individual corneal stroma during FACS analysis. **(C)** Representative contour FACS plots show the gates employed to detect the frequency of leukocyte (CD45) subsets expressing CXCR4 in an individual corneal stroma. The arrows point towards the population derived from the respective parent gate population. **(D)** Representative FACS plots showing CD31 expressing cells among CD45-ve cells in an individual corneal stroma and CD31+CXCR4+ expressing vascular endothelial cells. **(E)** Histogram Scatter plot denotes the frequency of myeloid cells and T cells among CXCR4+ leukocytes in the CS of the HSK corneas at 16-day p.i. A total of seven HSK corneas are processed for flow cytometry at 16-day p.i. Non-parametric Mann-Whitney's test was used to calculate the statistical significance (***$p<0.001$).